Atmos. Meas. Tech., 4, 1445–1461, 2011
www.atmos-meas-tech.net/4/1445/2011/
doi:10.5194/amt-4-1445-2011


Atmospheric Measurement Techniques

# A sublimation technique for high-precision measurements of $\delta^{13}CO_2$ and mixing ratios of $CO_2$ and $N_2O$ from air trapped in ice cores

**J. Schmitt**[1,2], **R. Schneider**[1], **and H. Fischer**[1,2]

[1]Climate and Environmental Physics, Physics Institute, & Oeschger Centre for Climate Change Research, University of Bern, Sidlerstrasse 5, 3012 Bern, Switzerland
[2]Alfred Wegener Institute for Polar and Marine Research, Bremerhaven, Germany

Received: 17 February 2011 – Published in Atmos. Meas. Tech. Discuss.: 16 March 2011
Revised: 6 July 2011 – Accepted: 11 July 2011 – Published: 19 July 2011

**Abstract.** In order to provide high precision stable carbon isotope ratios ($\delta^{13}CO_2$ or $\delta^{13}C$ of $CO_2$) from small bubbly, partially and fully clathrated ice core samples we developed a new method based on sublimation coupled to gas chromatography-isotope ratio mass spectrometry (GC-IRMS). In a first step the trapped air is quantitatively released from ∼30 g of ice and $CO_2$ together with $N_2O$ are separated from the bulk air components and stored in a miniature glass tube. In an off-line step, the extracted sample is introduced into a helium carrier flow using a minimised tube cracker device. Prior to measurement, $N_2O$ and organic sample contaminants are gas chromatographically separated from $CO_2$. Pulses of a $CO_2/N_2O$ mixture are admitted to the tube cracker and follow the path of the sample through the system. This allows an identical treatment and comparison of sample and standard peaks. The ability of the method to reproduce $\delta^{13}C$ from bubble and clathrate ice is verified on different ice cores. We achieve reproducibilities for bubble ice between 0.05 ‰ and 0.07 ‰ and for clathrate ice between 0.05 ‰ and 0.09 ‰ (dependent on the ice core used). A comparison of our data with measurements on bubble ice from the same ice core but using a mechanical extraction device shows no significant systematic offset. In addition to $\delta^{13}C$, the $CO_2$ and $N_2O$ mixing ratios can be volumetrically derived with a precision of 2 ppmv and 8 ppbv, respectively.

*Correspondence to:* J. Schmitt
(schmitt@climate.unibe.ch)

## 1 Introduction

$CO_2$ concentration measurements on polar ice cores provide direct atmospheric information of past carbon dioxide concentrations over up to the last 800 000 years (Fischer et al., 1999; Petit et al., 1999; Monnin et al., 2001; Ahn and Brook, 2008; Lüthi et al., 2008). Knowing the underlying natural causes of these $CO_2$ changes is key to predict its future dynamics. Therefore, refining our quantitative understanding of the observed glacial/interglacial variations in atmospheric $CO_2$ mixing ratio of about 100 ppmv, but also smaller variations during the Holocene, is an ongoing task of outstanding importance for the paleo climate community (Indermühle et al., 1999; Trudinger et al., 1999; Brovkin et al., 2002; Broecker and Clark, 2003; Köhler and Fischer, 2004; Elsig et al., 2009; Lourantou et al., 2010b). An important constraint on past changes in the global carbon cycle is the carbon isotopic signature of $CO_2$ ($\delta^{13}C$, with $\delta^{13}C = [(^{13}C/^{12}C)_{sample}/(^{13}C/^{12}C)_{reference} - 1] \times 1000$). However, the data coverage of $\delta^{13}C$ measurements is still fragmentary due to methodological limitations; i.e. measurements were done on selected time intervals, using different ice cores and different extraction devices, and in some cases precision is not sufficient (Leuenberger et al., 1992; Francey et al., 1999; Indermühle et al., 1999; Smith et al., 1999; Elsig et al., 2009; Lourantou et al., 2010a,b; Schaefer et al., 2011). $CO_2$ and $\delta^{13}C$ measurements usually use dry mechanical extraction (ball mills, needle crackers, cheese graters etc.) to release the air from gas enclosures in the ice. However, wet extraction methods, often used for other atmospheric trace gases, such as $CH_4$, might lead to $CO_2$ production within

Published by Copernicus Publications on behalf of the European Geosciences Union.

the melt water due to acid/carbonate reactions (Kawamura et al., 2003). Also the high solubility of $CO_2$ connected with a strong isotopic fractionation during gas-liquid transfer from the aqueous $HCO_3^-/H_2CO_3$ system limits the applicability of wet extraction methods for $CO_2$ (Anklin et al., 1995; Zhang et al., 1995). The dry extraction methods, however, suffer from rather low extraction efficiencies, ranging from only 50 % for fully clathrated ice to up to 90 % for bubble ice (Etheridge et al., 1988; Ahn et al., 2009; Lüthi et al., 2010; Schaefer et al., 2011). Note within this paper the term extraction efficiency refers to the efficiency during the actual extraction process, i.e. the release of enclosed gases from the ice sample. It does not include "post-extraction steps", like removal of the water vapor or the transfer of gas from the extraction line to the detection system. Extraction efficiency becomes important for ice from the bubble/clathrate transition zone (BCTZ), where fractionation between different gas species during the bubble clathrate phase transition has been observed (Ikeda et al., 1999; Lüthi et al., 2010). It becomes also crucial for high precision measurements of $\delta^{13}C$ from partly or fully clathrated ice. Here, dry extraction methods are only able to extract the $CO_2$ from opened bubbles and decomposing clathrates, where fractionation processes may come into play during the clathrate relaxation process. However, for $CO_2$ it is currently not clear if the observed gas fractionation during dry extraction is associated with a significant isotopic fractionation. A recent study using a ball mill dry extraction technique compared $\delta^{13}C$ values from two ice cores with either bubbly ice or ice from the BCTZ (Schaefer et al., 2011). While the authors also discuss other effects like ice microfractures and uncertainty from the gravitational correction being the culprit, ice from the BCTZ resulted in a larger scatter for $\delta^{13}C$ and showed a small but significant offset compared to bubbly ice of the same age interval. Accordingly, an extraction method achieving essentially 100 % extraction efficiency provides the best conditions to reliably decipher the carbon isotopic composition of $CO_2$ for clathrated ice, which covers most of the time span archived in deep Antarctic ice cores. In summary $\delta^{13}C$ measurements using dry extracted air from the BCTZ and clathrate ice are potentially vulnerable to larger systematic and stochastic errors. The only extraction technique for $CO_2$ from ice core samples which enables 100 % extraction efficiency is sublimation under vacuum. Several attempts to apply such a sublimation technique for concentration measurements of greenhouse gases have been undertaken during the last decades (Wilson and Long, 1997; Güllük et al., 1998). Although the sublimation apparatus designed by Güllük et al. (1998) was improved by Siegenthaler (2002), the resulting $CO_2$ data still showed a higher scatter and were less precise than the conventional mechanical crushing method (Siegenthaler, 2002). No attempts to measure $\delta^{13}C$ using sublimation extraction have been conducted so far.

Another issue with respect to $\delta^{13}C$ measurements regards the limited sample size available from ice cores. In earlier attempts, large sample sizes of up to 1 kg were needed applying the dual inlet technique (Leuenberger et al., 1992; Francey et al., 1999; Smith et al., 1999). This technique allows for a precision of ∼0.05 ‰ but with the drawback of high sample consumption. This poses serious limitations in creating highly resolved records in deep ice cores with thin annual layers and strongly limited ice core availability. Furthermore, contamination with drilling fluid caused some erroneous measurements as observed by Eyer (2004) and observations by H. Fischer during measurements on Taylor Dome ice. Here we present a new sublimation extraction-GC-IRMS technique which enables high precision measurement of $\delta^{13}C$ together with $CO_2$ and $N_2O$ mixing ratios on 30 g of both bubble and clathrate ice (equivalent to air samples of only 2–3 ml STP (standard temperature and pressure; 20 °C and 1 atm)). In contrast to the dual-inlet analysis, sample consumption is considerably reduced by a factor of more than 10 using the continuous flow inlet technique. In addition, an efficient gas chromatographic sample clean-up is possible removing the drilling fluid contamination and the isobaric component $N_2O$. Since the gas extraction from the ice is by far more time consuming than the actual IRMS measurement, the system was split into two separate lines. This allows to measure many extracted gas samples within a short time span and, thus, to take advantage of identical measurement conditions in the IRMS for a large set of samples. This is crucial as changes in the performance of the IRMS measurement, like source tuning, variations in the $H_2O$ background are a common problem. Following this technical partition, we first show the setup of the "sublimation system" and then the "tube cracker-GC" as the inlet system to the mass spectrometer. Subsequently, the referencing strategy, systematic corrections applied to the data and the performance of the analytical method on air samples and different kind of ice core sample types are discussed. In addition, we compare our data with previous results from other methods to evaluate the absolute accuracy of the measurements.

## 2 Experimental setup

### 2.1 General layout

The challenge to measure $\delta^{13}C$ at high precision together with the $CO_2$ mixing ratio on small ice samples led to the development of two separate preparation systems (Figs. 1 and 2 show the sublimation system, Fig. 3 the "tube cracker-GC" inlet). With the sublimation system (Figs. 1 and 2) an ice sample of ∼30 g is continuously sublimated. $CO_2$ (together with $N_2O$ and organic impurities) is cryogenically separated from the major air components ($N_2$, $O_2$ and Ar). After the sublimation of the ice sample is finished, the trapped fraction ($CO_2$, $N_2O$ and organic impurities such as components of the drill fluid) is transferred into a small glass tube (Fig. 4). In parallel, the corresponding total air content is determined

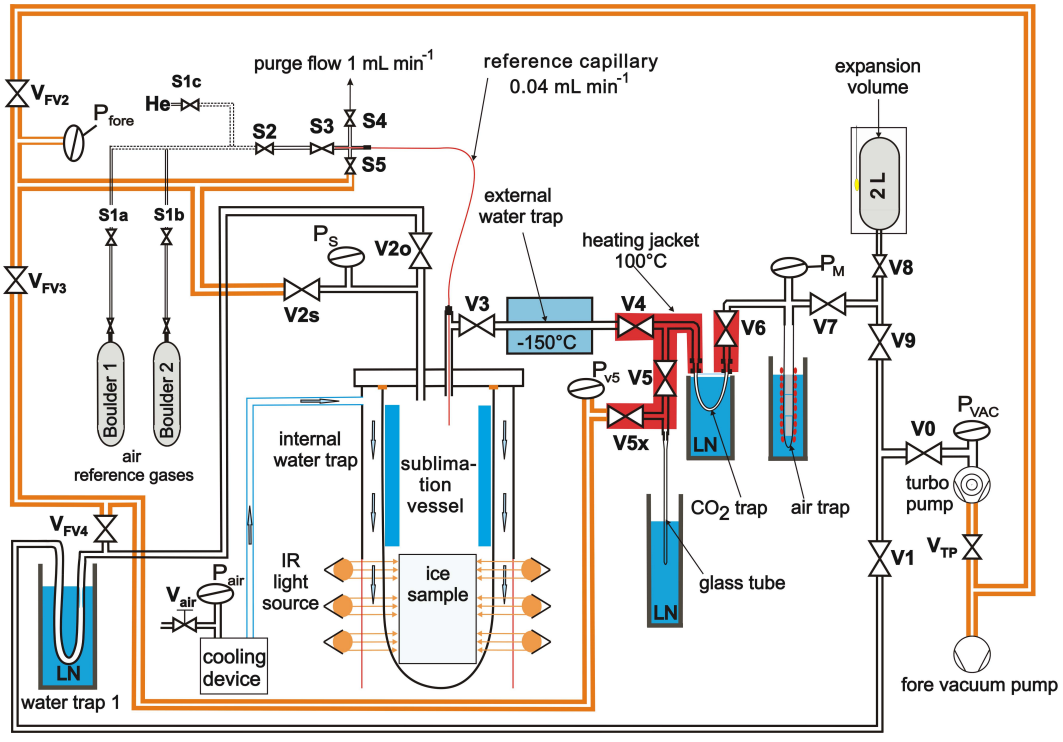


**Fig. 1.** Schematic view of the vacuum sublimation system. The sublimation vessel including the ice sample is cooled via a cold air stream supplied by the "cooling device". The released atmospheric gases from the sample are separated and collected in the $CO_2$ trap and air trap (right side). Reference air can be admitted during the sublimation of gas free blank ice via a fused silica capillary to provide identical conditions for sample and reference (top left).

manometrically. From this, the mixing ratios of $CO_2$ and $N_2O$ are calculated using the peak area provided by the mass spectrometric measurement. Although the sublimation step takes about one hour, the overall processing time is about 4 h, which limits our sample throughput to two samples per day. For the GC-IRMS measurement, the tubes are opened within a miniature cracker and the gas sample ($CO_2$, $N_2O$ and impurities) is transferred into a He carrier stream (Fig. 3). In a first step, the helium stream is dried, then the sample gases are cryofocused, finally a pulse of gas is transferred to a GC column, where the components are separated. The purified $CO_2$ is admitted to the IRMS via an open split. Both systems are equipped with "reference devices" to either introduce air standards or a $CO_2/N_2O$ mixture in helium, thus, to mimic the ice sample's way through the various analytic steps.

## 2.2 Sublimation system

### 2.2.1 General remarks

Degassing of $CO_2$ from O-rings, polymer based valves and seals and from glass and metal surfaces from the apparatus itself, are the main sources of contamination, which reduce measurement precision (Güllük et al., 1998; Siegenthaler, 2002; Elsig, 2009). As a consequence, our system was constructed to minimize the total surface of the system. Moreover, to reduce out-gassing further, polymer based O-rings or valves were excluded and only metal seals and valves are used. All valves which are in contact with sample $CO_2$ are all-metal valves (1/4″, Fujikin, FUDDFM-71G-6.35, Japan).

The improvements of the original Güllük apparatus by Siegenthaler reduced the total volume of this sublimation line to 1730 ml, whereas our design allowed a further reduction to ∼200 ml (for convenience, volume is used as a rough estimate for surface area). Since their sample size is comparable to ours, we achieved a considerable reduction of the active surface area of the sublimation line exposed to the sample volume. The main improvement was to merge the sublimation vessel and the bulky outer water trap into one vessel. Figure 2 shows the combined sublimation-water trap vessel. This single vessel design required a new cooling strategy using cold air as cooling agent.

### 2.2.2 Sublimation apparatus

The high vacuum within the sublimation line is provided by a turbo molecular pump backed by a rotary vane vacuum pump (both Leybold Vacuum, Germany). A large, 1/2″ diameter water trap (Fig. 1, "water trap 1") held at liquid nitrogen

**Fig. 2.** Photo showing the sublimation vessel with a loaded ice sample and the infrared source. The cooling jacket starts just above the ice sample and a cold air stream is fed in from both sides. The infrared source consists of 18 bulbs mounted on a holder, and the red UV filter visible in the central part. For the sublimation of the ice sample the infrared source is moved upwards, hence the section with sample is surrounded by the bulbs.

temperature is inserted between the sublimation line and the vacuum pumps to prevent $H_2O$ from entering the high vacuum side. The main advantage of our approach lies in the compact design combining the sublimation of the ice and the close-by removal of the bulk water vapour into one single vessel (33 mm o.d., 121 mm length, CF flange, Caburn, UK) shown in Figs. 1 and 2. The cooled upper part of the sublimation vessel is termed internal water trap. The compact design results in two benefits: First, the total surface area is reduced and the number of potentially leaky seals or connections is kept at a minimum. Secondly, it allows fast sublimation rates at low temperature and, thus, low water vapour pressure due to the large cross section of the sublimation vessel providing a high conductance. Consequently, the pressure and temperature difference between the ice sample and the condensed ice in the internal water trap a few cm above is small. This is mandatory to achieve a high sublimation rate at low temperature to keep the ice surface well below $-20\,^{\circ}C$. Above this temperature, a quasi-liquid layer might form on the ice surface allowing chemical reactions to take place (Güllük et al., 1998; Barnes et al., 2003).

An air stream of $-115\,^{\circ}C$ directed by a cooling jacket allows the upper zone of the sublimation vessel, i.e. the internal water trap, to be cooled to the desired temperature. The sublimation is run at around 0.25 mbar $pH_2O$ or $-34\,^{\circ}C$. The pressurised air is cooled via a copper heat exchanger mounted in a 2-l Dewar ("cooling device" in Fig. 1). Liquid nitrogen (LN2) is automatically pumped from a reservoir into this heat exchange Dewar until the temperature set-point is reached, with the temperature of the air flow regulated by a thermocouple and a proportional-integral-derivative (PID) controller (West 2300, UK). Although the design of this LN2 pump is basic the resulting temperature of the cooling air can be adjusted fairly constant with changes being $<2\,^{\circ}C$ (Schmitt, 2006). The temperature of the cooled air stream can be continuously adjusted from ambient temperature to a lower limit of $-150\,^{\circ}C$, where the system becomes unstable due to condensation of $O_2$. Via a flow regulator valve and a manometer ($V_{air}$ and $P_{air}$, Fig. 1) the flow is adjusted to the required demand of coolant from 0 to $\sim 50\,l\,min^{-1}$, corresponding to a maximum cooling capacity of $\sim 100$ W (with a $\Delta T$ of $\sim 100\,^{\circ}C$ between the cold air stream and the glass vessel). Primarily, the air stream has to remove the latent heat released during the deposition of the water vapour on the wall of the sublimation vessel ($\sim 30$ W) and secondly to cool the lower part of the glass vessel which absorbs long-wave radiation. Infrared light from halogen bulbs, which surround the sublimation vessel (18 bulbs each with max 30 W at 12 V, Microstar, Osram, Germany) provides the energy for sublimation (Figs. 2 and 3). As the absorption coefficient of ice below 600 nm is small, only the long wave part ($\lambda > 600$ nm) of the emitted spectrum is used for the sublimation. Additionally, the emitted light is passed through a special foil filter (Colour Foil, No. 105 orange, LEE, Germany), absorbing the short wave light ($<600$ nm). Removing the short wave part is a precautionary measure to get rid of the UV part, which could potentially interfere with organic impurities within the ice to produce in-situ $CO_2$.

The flange head has two 1/4″ feedthroughs, which are connected to the 1/4″ tubing (Fig. 1). The left feedthrough is connected to a pressure transducer, "$P_S$" (1 Torr max, Leybold Vacuum, Germany), to control the $H_2O$ vapour pressure and, thus, temperature during the sublimation. Via valve V2s, the sublimation vessel can be connected to the forevacuum to evacuate the sublimation vessel after opening it to load the ice sample. Via valve V2o, the sublimation vessel

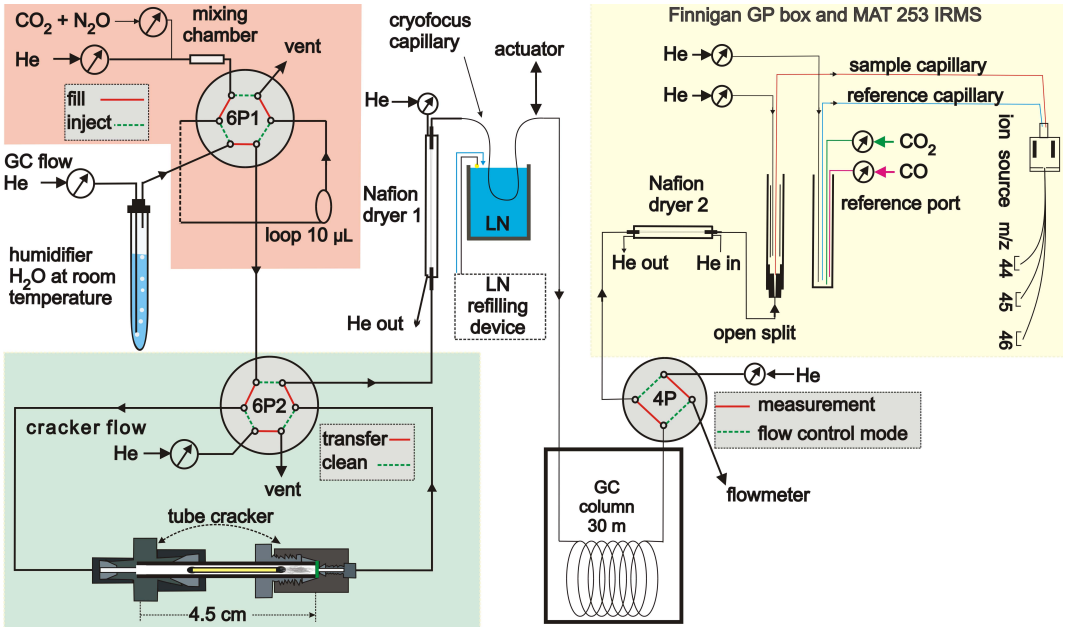


**Fig. 3.** Flow scheme of the tube cracker-GC-IRMS line with a device to introduce $CO_2/N_2O$ pulses into the GC carrier gas (red box), the tube cracker (green box), followed by a Nafion dryer, cryofocus capillary, GC, 2nd Nafion dryer and finally the inlet system with the open split leading to the ion source of the IRMS and the reference port to inject $CO_2$ std/on off peaks and to admit a continuous CO background (yellow box).

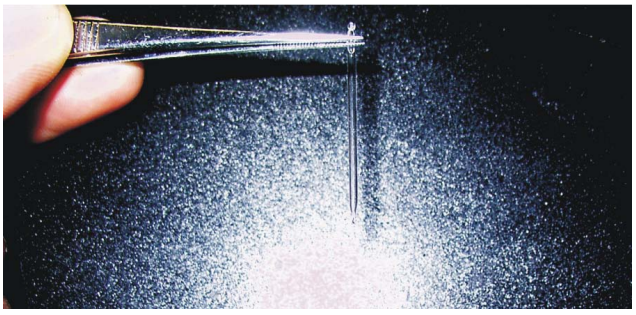

**Fig. 4.** Photo showing the closed sample tube.

can be connected to the turbo pump, passing water trap 1 (with $V_{FV4}$ closed). Onto the right feedthrough, an inlet capillary is mounted which allows the continuous introduction of reference air (see section on air reference inlet). Via valve V3, the sublimation vessel is connected to the external water trap and the consecutive traps.

### 2.2.3 External water trap

Although the internal water trap already removes 99 % of the water vapour, an additional, external water trap was needed to achieve the requirements for extreme low $pH_2O$ in the final $CO_2$ sample. A compact water trap to minimize the total surface area of the system was aimed at. Since in our application the trapped $CO_2$ and with it any $H_2O$ traces are ultimately transferred into a miniature glass capillary with a volume of only 15 µl, a $H_2O$ amount of just 0.1 µg is sufficient to form a liquid phase. In case the $H_2O$ flux exceeds 0.1 µg, liquid $H_2O$ forms within the tube after the transfer from the $CO_2$ trap to the glass capillary and warming to ambient temperature. The presence of a liquid phase within the tube allows $CO_2$ to exchange oxygen with $H_2O$. This shifts the $\delta^{18}O$ values to more depleted values of up to 5 ‰ depending on the $\delta^{18}O$ value of the ice sample. Therefore, temperatures as cold as −150 °C in the external water trap are needed to reach the required $H_2O$ vapour pressure. Since classical cooling systems, e.g. dry ice/pentane slush (Leckrone and Hayes, 1997) are not readily suitable for this temperature range and closed-cycle He coolers are too bulky, we constructed a trap to match our requirements. The trap is made of silitec coated stainless steel tubing (Restec, USA) with 1/4″ o.d., 0.53 cm i.d., 20 cm length to reduce adsorption of $CO_2$ on the cold surface of the trap. This tubing rests within an aluminium block, which is cooled with LN2 droplets and cold nitrogen gas; for details see Schmitt (2006) and Bock et al. (2010). A second reason for the usage of a LN2 cooled water trap is the general exclusion of solvents within our laboratory as traces of organic contaminants are reported to interfere with the IRMS measurement due to isobaric interferences (Francey et al., 1999; Leuenberger et al., 2003; Eyer, 2004). The temperature of the trap is automatically controlled via a thermocouple and a PID controller with an output current driving the “LN2 pump” similar to the air

cooling system of the sublimation vessel. Since the trap is operated only 25 °C above the corresponding $CO_2$ saturation pressure during sublimation conditions ($p_{air} = 0.1$ mbar with $p_{CO_2} \sim 2.8 \times 10^{-5}$ mbar), cold spots in the trap are of special concern. To detect potential cold spots, we tested the trap by filling it with $CO_2$ at 0.001 mbar and held the trap at −150 °C for 10 min to observe a pressure drop due to condensation or adsorption. Within the range of precision of the pressure measurement no loss of $CO_2$ was observed, thus, we are confident that the trap shows no cold spots.

#### 2.2.4 $CO_2$ trap and glass capillary

From the dried air stream provided by the external water trap, the $CO_2$ trap removes $CO_2$, $N_2O$ and organic impurities from the bulk air ($O_2$, $N_2$, Ar), which is adsorbed in the consecutive air trap. The $CO_2$ trap is a 8 cm long, U-shaped, 1/8″ stainless steel tubing which can be immersed in a dewar filled with LN2 during the trapping procedure (Fig. 3 shows the $CO_2$ trap in immersed position). After sample collection, the $CO_2$ trap can be rapidly heated to transfer the gases into the glass capillary. For this, a heating jacket is wrapped around the $CO_2$ trap to allow heating the trap from −196 °C to +100 °C within 50 s. The tubing and valves enclosed between V4–V5x and V6 (red area in Fig. 1) are permanently heated to 100 °C to minimise $CO_2$ adsorption during the transfer of the $CO_2$ to the glass tube.

The tip of an ordinary Pasteur glass pipet is used to collect and store the extracted $CO_2$. Prior to usage the glass capillaries are cleaned in an ultrasonic bath with diluted HCl and thoroughly rinsed with deionised water to eliminate organic and inorganic contaminants from the glass surface. The capillary's tip is flame sealed and the diameter of the open end (3 mm o.d.) is adjusted and rounded with a hand torch to fit into the 1/8″ o.d. Cajon-Ultratorr adapter with which the glass tube is connected to the $CO_2$ trap via V5. To pump off the atmospheric air from the glass tube and tubing, valve V5x can be connected to the fore-vacuum or after checking the pressure at $P_{V5}$ to the high vacuum ($V_{FV4}$ open, $V_{FV3}$ closed).

#### 2.2.5 Air reference inlet

The prerequisite of accurate measurements for isotope analysis is the so called principle of "Identical Treatment" (IT) coined by Werner and Brand (2001). To perfectly fulfil this requirement, one would need artificial ice with air inclusions of known composition. As such a reference material is not available the second best referencing strategy is to continuously admit an air reference during the sublimation of gas free ice ("blank ice"). This treatment mimics the air release from the sample during the sublimation as closely as possible. Except for the actual gas release from the ice surface and possible impurities, all subsequent steps are then identical for reference and sample. For referencing we use two pressurised air cylinders with known $\delta^{13}C$ values and known atmospheric mixing ratios for $CO_2$ and $N_2O$. These two air cylinders contain current atmospheric air, with $CO_2$ mixing ratios being reduced to obtain $CO_2$ mixing ratios covering the minimum and maximum values during the last 800 ka years. Cylinder CA06195 ("Boulder 1") has a $CO_2$ mixing ratio of $182.09 \pm 0.04$ ppmv, $\delta^{13}C$ of $-7.92$ ‰ $\pm 0.003$ ‰ with respect to VPDB-$CO_2$ (the international reference material Vienna Peedee belemnite) and $\delta^{18}O - 4.756$ ‰ $\pm 0.007$ ‰ with respect to VPDB-$CO_2$. Cylinder CA06818 ("Boulder 2") has a $CO_2$ mixing ratio of $296.80 \pm 0.02$ ppmv, a $N_2O$ mixing ratio of $263.4 \pm 3.7$ ppbv, $\delta^{13}C$ of $-8.421$ ‰ $\pm 0.003$ ‰ with respect to VPDB-$CO_2$ and a $\delta^{18}O - 4.800$ ‰ $\pm 0.014$ ‰ with respect to VPDB-$CO_2$. The two cylinders and the values given above were obtained by the Stable Isotope Lab (SIL) at the Institute for Arctic and Alpine Research (INSTAAR), University of Colorado, in cooperation with the Climate Monitoring and Diagnostics Laboratory (CMDL) of the National Oceanic and Atmospheric Administration (NOAA).

Since the gas release during sublimation is a continuous but slow process, a reference inlet was needed to allow a constant flow of air into vacuum conditions without fractionation and, thus, to mimic the gradual air release during the ice sublimation process. Our reference gas inlet system consists of three components (Fig. 1): (1) the pressurised air cylinders with pressure regulators representing the reference gas supply, (2) an inlet capillary through which a defined amount of air enters the extraction vessel, (3) a vent capillary to keep the system well flushed. The pressure of the inlet capillary can be adjusted from 100 to 350 kPa with a pressure regulator (0–100 psi, Air Gas, USA), to span the gas release rates during the sublimation of samples (0.02 to 0.06 ml STP $min^{-1}$). The inlet capillary has an i.d. of 0.05 mm and provides a viscous flow regime at this pressure range. The outlet of this capillary is some mm above the ice cube surface to achieve similar flow and mixing conditions of gas and water vapour. The flow rate of typically 0.04 ml STP $min^{-1}$ through this inlet capillary is far too low to flush the reference system efficiently, a prerequisite for stable measurements. Otherwise long lasting drift phenomena for $\delta^{13}C$ and $CO_2$ and bad reproducibility would result. Therefore, the reference system is equipped with a purge valve ("S4") directing a higher flow of approx. 1 ml STP $min^{-1}$ at 200 kPa to a vent capillary (fused silica, 0.05 mm i.d., 15 cm) with which the system can be continuously flushed during operation. The inlet system is connected to the vacuum system via S5, which is closed when reference gas is admitted to the sublimation vessel. For ice core samples S5 has to be opened to evacuate the inlet system, while S4 and S3 are closed. With this reference inlet, air is admitted during the sublimation of blank ice to achieve identical treatment of sample and reference. Consequently, however, only the same throughput like for the real ice samples is achieved this way, i.e. at best two samples a day. When the sublimation device is not used the air

reference inlet is flushed with helium via valve S1c while S4 and S6 are closed.

#### 2.2.6 Volumetric determination of mixing ratios

Although the main purpose of the system lies in the precise determination of $\delta^{13}C$, it is crucial to measure the mixing ratio of $CO_2$ and $N_2O$ on the same ice sample with high precision, because: (1) a significant deviation in the $CO_2$ mixing ratio from neighbouring samples or from different extraction techniques is a valuable tool to detect contamination or loss processes during the whole analysis. (2) For a quantitative interpretation of global atmospheric $\delta^{13}C$ changes with models, it is imperative to have the data of both the isotopic and the mixing ratio at the same time interval. Although highly resolved time series on $CO_2$ mixing ratio are available for the Holocene (Etheridge et al., 1996; Monnin et al., 2001; Siegenthaler et al., 2005a; MacFarling Meure et al., 2006), temporal resolution is yet poor during MIS3 and older periods and dating uncertainties as well as a mismatch in the gas age–ice age difference of different cores weaken the precision necessary to disentangle global carbon fluxes. (3) Diffusion and fractionation processes in the transformation zone between bubble and clathrate ice and below call for extraction techniques which allow 100 % extraction efficiencies to provide unfractionated $CO_2$ concentrations and to validate the measurements on such ice using the classical dry extraction techniques (Lüthi et al., 2010).

With the mass spectrometer providing the amount of $CO_2$ via the peak area, the amount of the corresponding air is volumetrically determined from the collected gases in the air trap. For this we use a glass tube (1/4″ o.d., 1/8″ i.d.) filled with 5 Å molecular sieve in pellets (diameter 5 mm, length 20 mm). Before usage and for weekly regeneration, water is removed by heating the molecular sieve to 140 °C for a few hours. During the sublimation, the air trap is immersed into LN2 and acts as a vacuum pump. At −196 °C the equilibrium air pressure above the loaded molecular sieve (2 ml STP air) is <0.0020 mbar ("$P_M$" pressure transducer, $10^{-4} - 1$ Torr max). It is therefore the molecular sieve that drives the pressure gradient from the sublimation vessel through the external water trap and $CO_2$ trap to the air trap, thus acting as a cold finger. The quantitative release of the adsorbed gases is accomplished by heating the trap to +100 °C. The desorbed air components are expanded into a 2-l expansion volume which is thermally insulated to get a stable temperature reading. After pressure stabilizes within the system, the final pressure and temperature of the expansion volume are read out.

### 2.3 Tube cracker GC system

#### 2.3.1 General remarks

Tube cracker applications are used in many fields of isotope analysis for many decades. Usually, a glass tube containing the extracted gas sample acts as the interface coupling a separate sample preparation step to the isotopic measurement at the dual inlet IRMS. Tube outer diameter dimensions normally used with the latter techniques are 1/4″ or even 3/8″ and the gas is expanded into the bellow or cold finger of the MS after breaking the tube and before admitting it to the changeover valve. This direct route to the IRMS is not feasible for $CO_2$ samples from our ice core samples for three reasons. (1) Only small amounts of $CO_2$ are available since the amount of ice is limited and/or a high temporal resolution and replicates are preferred to get a robust record. (2) Precise $\delta^{13}C$ values on atmospheric $CO_2$ samples containing $N_2O$ either involve a mathematic correction for isobaric interference, or the separation of both gases via chromatography (Ferretti et al., 2000). (3) The most important reason for a gas chromatographic separation step prior to the IRMS measurement is organic contaminants which can interfere in the MS measurement: traces of drilling fluid, which often accompany deep ice core samples, were occasionally observed on the Taylor Dome ice core during the measurements of the data set for Smith et al. (1999) and on Dome C ice by Eyer (2004). Interferences with the solvent ethanol were reported by Francey et al. (1999) and Elsig (2009) reported contamination from an unknown organic released during the mechanic extraction process. Since some organic components, like the drilling fluid, behave physicochemically similar to $CO_2$ during the extraction process, minute traces of this substance can simultaneously reach the ion source if not separated before. We observed such problems during earlier measurements of drill fluid contaminated ice core samples, which manifested themselves by excessively high *m/z* 45 and 46 traces yielding highly enriched $\delta^{13}C$ ratios (>1000 ‰). Note, all measured ice cores in this study used a drill liquid consisting of two components: The densifier HCFC-141b, 1,1-dichloro-1-fluoroethane, and Exxsol D30, a mixture of hydrocarbons (Augustin et al., 2007). It is likely that HCFC-141b causes the interference on *m/z* 45, as this mass is one of the main fragments during the ionisation of this molecule (http://webbook.nist.gov). Additionally, HCFC-141b has a lower boiling point (32 °C) compared to Exxsol D30 (100 °C–150 °C), thus, traces of the densifier vapour are likely to pass the cold region (−150 °C) of the external water trap. Indeed, at −150 °C the saturation vapour pressure of HCFC-141b is still $1.5 \times 10^{-5}$ mbar (extrapolation of data from http://webbook.nist.gov), thus comparable to the partial pressure of $CO_2$ with $2.8 \times 10^{-5}$ mbar calculated for the conditions within the external water trap. Consequently, HCFC-141b is able to pass the cold region of the external water trap.

Our cryofocus and GC separation avoids these contamination issues. Although a severe contamination can easily be detected by unusual, or physically or climatologically unrealistic $\delta^{13}C$ values and excluded from the data set, minor contaminations are more difficult to detect and require many replicates or a comparison of different cores. In conclusion, gas chromatographic separation of $CO_2$ from $N_2O$ and organic impurities is indispensable. From this follows the special design of our CF–IRMS application consisting of an injection port for a $CO_2/N_2O$ mixture, a flow-through tube cracker, a Nafion dryer, a cryofocus, a gas chromatograph and a $2^{nd}$ Nafion dryer (Fig. 2). Our system is linked to a MAT 253 via the open split of a conventional Precon GP-box system (Thermo Electron, Bremen). The components with their special features are described in detail in the following sections.

### 2.3.2 $CO_2/N_2O$ injection device

To fulfil the requirement of identical treatment of sample and reference within the cracker-GC-IRMS system (Fig. 3), a device was constructed allowing $CO_2/N_2O$ pulses to be injected into the cracker with a 10 µl loop attached via the "SP1" six-port valve (Valco, USA). The $CO_2$ and $N_2O$ concentration can be adjusted to appropriate values ($\sim$4 % $CO_2$ in He, or $\sim$8 nmol absolute per 10 µl filling) by dilution of $CO_2$ and $N_2O$ with He in a mixing chamber. The $CO_2$ used for these pulses is identical to our monitoring gas and has a $\delta^{13}C$ of $-4.48$ ‰ with respect to VPDB and a $\delta^{18}O$ of $-19.89$ ‰ with respect to VPDB. With two pressure regulators (Porter 8286-SMVS-30, USA) the flow rate is set to $\sim$0.1 ml min$^{-1}$ for the $CO_2/N_2O$ mixture and 15 ml min$^{-1}$ for helium. This mixing device allows a convenient adjustment of the signal height of the $CO_2$ peaks without the need to switch between different loop sizes. To introduce a $CO_2/N_2O$ pulse, the SP1 valve is switched to the "inject" position and the GC flow (0.85 ml min$^{-1}$) flushes the $CO_2/N_2O$ mixture from the 10 µl loop via the "6P2" valve to the cracker device (Fig. 3).

### 2.3.3 Cracker

Instead of the $CO_2/N_2O$ pulses described above, a sealed sample tube containing the trapped $CO_2$-$N_2O$ mixture from an ice core sample can be introduced via the cracker device. The schematic layout of the cracker system can be seen in Fig. 3. The sealed tubes with the extracted $CO_2$ and $N_2O$ are mounted into a flow-through tube cracker. After flushing the cracker with helium, the tube is manually broken, its content is transferred out of the cracker passing a Nafion dryer and trapped on a cryofocus capillary. With an actuator the capillary is lifted out of the LN2 to release the trapped gases, which are then directed to a GC column, where $CO_2$ is separated from $N_2O$ and organic impurities before entering a continuous-flow isotope ratio mass spectrometer via an open split. A similar line for $\delta^{13}C$ determination at a precision of $<$0.05 ‰ was published earlier (Ferretti et al., 2000; Ribas-Carbo et al., 2002). The main difference is that a discrete amount of $CO_2$ ($\sim$20 nmol) enters our system via the special tube cracker device which allows us to achieve the same precision from only 2 ml STP compared to a total sample consumption of up to 45 ml from a large flask sample reservoir (Ferretti et al., 2000). To reduce the internal volume of the cracker to a minimum, the tube cracker is made of a 1/16–1/8″ o.d. Swagelok reducing union, a 4.5 cm 1/8″ o.d. stainless steel tubing, which is the flexible part and houses the glass tube, and a 1/8–1/16″ o.d. Valco column end fitting. This fitting is equipped with a 2-µm stainless steel frit to prevent glass particles from the cracker entering the down stream part and potentially clogging the valve. The total internal volume of the cracker is only 160 µl, and the sample is flushed with a He flow rate of only 0.85 ml min$^{-1}$ to the cryofocus capillary.

### 2.3.4 Humidifier

High precision $\delta^{13}C$ measurements require low and constant water levels within the ion source since $HCO_2^+$ production causes apparent sample enrichment (Leckrone and Hayes, 1998; Meier-Augenstein, 1999; Rice et al., 2001). Therefore, water vapour is generally kept at low levels within the carrier gas stream of CF-IRMS applications. Contrary to this common notion, a special humidifier device saturating the carrier gas with $H_2O$ had to be inserted prior to the tube cracker device and consecutively the $H_2O$ is removed again from the carrier via a Nafion dryer after passing the cracker. The reason for this unusual procedure was that although $CO_2$ pulses admitted to the cracker via the loop resulted in reproducible $\delta^{13}C$ values, similar measurements of $CO_2$ prepared in glass tubes revealed a serious fractionation with poor precision ($>$1 ‰). We found the cause of this problem to be a strong adsorption and fractionation occurring on the fresh glass surfaces after breaking the tubes in the cracker. To prove this, empty tubes were evacuated and sealed off at high vacuum. These tubes were then inserted into the cracker and a first measurement was conducted where a pulse of $\sim$8 nmol $CO_2$ from the loop was flushed to the cracker and flowing around the intact glass tube. A second $CO_2$ pulse was then admitted to the cracker with the empty tube broken prior to arrival of the gas at the crushed glass particles. Whereas no effect was visible in case of the intact tube, a strong fractionation occurred with the crushed tube. A considerable reduction of the peak area of up to 15 % was noticed, depending on the breaking conditions with more or less glass particles produced during the cracking. Moreover, for the isotopes, the $\delta^{13}C$ and $\delta^{18}O$ ratios were shifted by $\sim$+1 ‰ and $\sim$+2 ‰, respectively. From this we deduced, that a fractionating adsorption process occurs on the fresh glass surface. Although the tube cracker technique is well established for many decades (Des Marais and Hayes, 1976; Caldwell et al., 1983), this method

is generally applied for dual inlet-Multiport measurements with $CO_2$ amounts a factor of 100 larger than in our case.

Although the amount of glass particles can be considerably reduced by scoring the tube, this is not an easy task and not reliable enough due to the tiny dimensions of the capillary (1 mm o.d.). Consequently, the other possibility was to inhibit the $CO_2$ adsorption. This is done by providing a strong adsorbent in excess: water vapour. The helium flow of the GC carrier gas is bubbled through deionised water within a 1/4″ o.d. glass tube similar to the humidifier used by Leckrone and Hayes (1997). The excess of $H_2O$ compared to $CO_2$ (molar ratio $H_2O/CO_2$ ∼20 within the cracker) then prevents $CO_2$ from adsorbing at the glass surfaces, accordingly, the fractionation phenomenon disappeared after installation of the humidifier. After the cracker an extra long Nafion dryer is needed again to remove the high load of water vapour before the He stream enters the cryofocus capillary. We use a Nafion membrane (0.03″ o.d. and 50 cm length, Ansyco, Germany) housed in a 1/8″ o.d. glass tube and a counter current He stream of 5 ml $min^{-1}$ to dry the GC flow.

#### 2.3.5 Cryofocus, GC, IRMS injection

As cryofocussing capillary we use a loop of deactivated fused silica (0.32 mm o.d., 20 cm length) which can be immersed in LN2 by a pneumatic actuator. The sharp sample pulse from the cryofocus is directed to the GC, where separation of $CO_2$ from $N_2O$ and organic drilling contaminants is achieved at 110 °C using a GS-Carbonplot column (length 30 m, o.d. 0.32 mm, Agilent). Note that at this temperature the drilling fluid components are strongly retained on the GC column, thus, during the IRMS measurement we do not observe a separate peak from these compounds. These compounds are only removed at the high temperatures used in the stand-by mode at 200 °C. A sample chromatogram shows that $CO_2$ is sufficiently separated from $N_2O$ (Fig. 6a). An even better separation could be achieved using a lower GC temperature, however, this also results in a stronger separation of the $CO_2$ isotopologues, thus, increasing the time shift between *m/z* 44 and *m/z* 45 (Meier-Augenstein et al., 1996). Although this time shift can be accounted for by the software, we observed a stronger dependence of the isotopic ratio on the amount of the sample (usually referred to as linearity effects or amount dependency), a common phenomenon with GC-IRMS applications (Hall et al., 1999; Schmitt et al., 2003). Therefore, we choose a GC temperature of 110 °C, which results in a sufficient separation between $CO_2$ and $N_2O$ of 14 s (see Fig. 6a) with still a moderate time shift of typically <0.1 s between the *m/z* 44 and *m/z* 45 beams. Nevertheless, we usually observe a small amount dependency of the measured $\delta^{13}C$ values, which has to be corrected for (see section $\delta^{13}C$ correction).

Finally, the $CO_2$ and $N_2O$ peaks pass the 2nd Nafion dryer and are transferred to a modified GP-Interface (Thermo Electron, Bremen, Germany) to be admitted to the ion source of the MAT 253 via the open split and inlet capillary with a flow rate of ∼0.3 ml $min^{-1}$ STP.

Via the reference port and reference capillary (Fig. 3) we continuously introduce a small amount of carbon monoxide (∼200 mV for *m/z* = 28 on the major cup with the standard resistor of $3 \times 10^8\ \Omega$) to reduce adsorption-desorption effects of $CO_2$ at the surfaces of the ion source (Elsig and Leuenberger, 2010).

## 3 Analysis procedure

### 3.1 Sample preparation and sublimation

Prior to the sublimation of an ice sample, each ice cube has to be prepared in the following way to provide a clean surface. With a band saw a cube is cut to the dimensions 3.5 cm × 3.5 cm with 4.5 cm length. To fit this cube into the sublimation vessel with an internal diameter of 3.3 cm, the edges are rounded and trimmed with a stainless steel knife to a cylinder of ∼3.2 cm diameter and a weight of ∼30 g. The ice is inserted in the precooled sublimation vessel which is mounted to the flange via a copper gasket. First the atmospheric air is pumped out of the vessel until a constant value is reached corresponding to the vapour pressure of the ice. Since $CO_2$ adsorption on the surfaces is a critical issue, two hours at vacuum to decontaminate the system is necessary. As pointed out by others, $CO_2$ desorption from surfaces is most effective at high $H_2O$ pressures (Zumbrunn et al., 1982; Güllük et al., 1998). With the cooling system, a temperature of ∼ −34 °C is adjusted within the vessel leading to a $pH_2O$ of ∼0.25 mbar (pressure transducer "$P_S$" in Fig. 1). If the system is leak free, a final pressure of $<2 \times 10^{-7}$ mbar is achieved at the high vacuum side with gas free blank ice and $\sim 5 \times 10^{-7}$ for bubble or clathrate ice due to slow sublimation of the ice, which releases some air. After two hours at vacuum, a few millimetres of ice have been removed and the surfaces of the vessel and the traps are sufficiently clean. The sublimation is started by increasing the current of the halogen bulbs and simultaneously decreasing the temperature of the cooling gas stream to −115 °C and adjusting its flow rate such that a $pH_2O$ of ∼0.25 mbar is obtained. Sampling is then started by cooling down the $CO_2$ trap and the air trap and opening V3. The steady gas stream liberated from the ice is now flowing towards the air trap. Collection of gas is stopped after 50 min by closing V3, V4 and V6 and cooling down the glass tube. After V5 is opened, the $CO_2$ trap is released from the LN2 Dewar and warmed up for 60 s and $CO_2$ is transferred from the trap to the glass tube. Finally, the glass tube is flame sealed and stored until the GC-IRMS measurement. Parallel to the last steps, the air trap is removed from LN2 as well and warmed to 100 °C. The air quantitatively desorbs from the molecular sieve and the constant pressure is read out at "$P_M$" (Fig. 1) to calculate the $CO_2$ and $N_2O$ mixing ratios.

Note, that only ∼85 % of the ice sample is sublimated during the 50 min duration leaving around 5 g of the ice sample in the vessel. A complete sublimation of the ice sample is not intended since ice impurities (mineral dust and organics) may gradually accumulate at the ice surface and could enhance chemical reactions when highly concentrated at the final stage. Additionally, the sublimation rate of the remaining ice piece is getting extremely slow and highly variable leading to scattered results. Regardless of this reasoning, leaving some ice unsublimated does not compromise our 100 % extraction efficiency, as the remaining ice stays entirely intact. This is different for conventional mechanical extractions, where initially the entire ice sample is crushed but the gas content is released only partially giving rise to fractionation of the measured mixing ratios for partially clathrated ice (Lüthi et al., 2010; Schaefer et al., 2011).

### 3.2 Cracker-GC-IRMS measurement scheme

The high precision attainable using dual-inlet IRMS is based on the direct comparison of sample and reference of similar signal amplitude. Gas is admitted to the ion source by identically crimped capillaries. In contrast, for continuous flow applications, this identical treatment of sample and reference is accessible only to a certain degree, e.g. by using an internal reference inlet (Meier-Augenstein, 1997). The favoured strategy is to bracket a sample peak with two references and try to adjust their signal heights as precisely as possible (Rice et al., 2001). For practical reasons, a precise adjustment is not completely possible, therefore the data has to be corrected using empirical functions for the amount dependency in $\delta^{13}C$ (see Sect. 4.2). Our strategy outlined here is based on two different sets of "referencing peaks". Air standards admitted to the sublimation vessel during the sublimation of blank ice offer by far the closest analogue to gas samples extracted from ice. Due to large effort to produce them, it is unfeasible to use this type of reference for all correction purposes. But they are the basis on which the samples are referred to in terms of absolute value of $\delta^{13}C$ and the mixing ratios of $CO_2$ and $N_2O$. In contrast, $CO_2/N_2O$ injections automatically admitted to the cracker system with subsequent cryofocusing and GC separation face the same treatment as sample tubes and feature their identical peak shape. With these $CO_2/N_2O$ injections the system's $\delta^{13}C$ drift with time and the dependence of $\delta^{13}C$ on the peak area ("linearity") are corrected for (see linearity section in Fig. 5). As pointed out above, identical measurement conditions are of paramount importance to obtain a high precision $\delta^{13}C$ record from the samples. Therefore, we extract the air from several ice core samples and store the $CO_2$ in glass tubes until they are all measured in a single run. A typical measurement session comprises up to 20 h, starting with a "linearity section" consisting of pairs of an "equilibration peak" (EQ) followed by a "linearity peak". The size of the "linearity peak" is varied to produce three different peak heights (L3, L2 and L1),

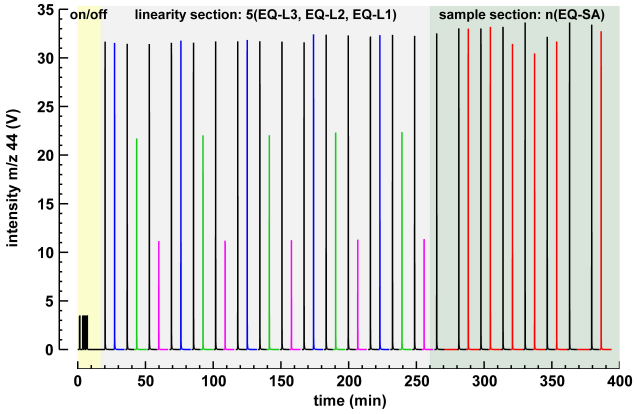


**Fig. 5.** Chromatogram showing the first 400 min of a typical measurement session comprising up to 1500 min. Within the first 10 min $CO_2$ pulses are introduced by the reference port of GP box (so called std on/off peaks). The "linearity section" runs from 15 min to 260 min, where pulses of a $CO_2/N_2O$ mixture are introduced into the tube cracker GC system. The "linearity peaks" are produced in three size classes, L3 in blue, L2 in green, L1 in magenta; each "linearity peak" is preceded by an "equilibrium peak", EQ in black. This scheme of EQ-L3, EQ-L2, EQ-L1 (= one block) is then repeated five times. In the following "sample section", starting at 260 min, the first eight measured sample tubes are shown (in red), with the sample 1 and sample 7 being empty tubes. Identical measurement conditions for each of these peaks are provided by an equilibration peak (EQ in black) preceding each of them. After all sample tubes have been processed, a second "linearity section", consisting of four blocks, followed by a series of std on/off closes the measurement session (not shown).

which can later be used to correct for amount effects. The injection of the $CO_2$-$N_2O$ mixture to the carrier gas stream is carried out by switching the valve "6P1", which injects ∼8 nmol $CO_2$ into the He stream. To produce linearity peaks with different peak sizes, the loop is filled and flushed out one, two or three times. A filling-injection cycle lasts for 3 s. Due to the cryofocus the peak shape for different sizes is identical for tube samples, which is a prerequisite for applying the identical treatment principle. The aim of preceding each "linearity peak" or sample peak with an equilibration peak (EQ) is to provide identical conditions by equilibrating both the cracker-GC system and the ion source prior to all samples. This alternating EQ-L3, EQ-L2, EQ-L1 scheme is repeated five times until the actual sample tubes (SA) are measured (sample section in Fig. 5). Again, an equilibration peak precedes each sample tube, leading to an alternating EQ-SA scheme. As the process is fully automated except for the tube cracker itself, only the opening/closing of the cracker and breaking the tube needs personal attendance.

To be loaded with a new sample tube, the cracker is opened and the glass shards of the last tube are removed. During that time the GC carrier flow (0.85 ml $min^{-1}$) bypasses the cracker via the "6P2" valve (Fig. 1), whereas the second

He flow (cracker flow: 5 ml min$^{-1}$) sweeps the atmospheric air out to the vent after the cracker is closed. Flushing the cracker lasts for 60 s, the "6P2" valve is then switched back and the GC carrier flows through the cracker again. Before the sample tube is processed further, the preceding equilibration $CO_2$ peak is prepared by switching the "6P1" valve three times, injecting in total 24 nmol $CO_2$ from the $CO_2$/$N_2O$ mixture. The injected mixture flows through the cracker to mimic the sample and then towards the cryofocus capillary immersed in LN2. After quantitative trapping (90 s) the capillary is lifted out of the LN2 and the sample directed to the GC where $CO_2$ is separated from $N_2O$. Via the open split, the $CO_2$ and $N_2O$ peaks enter the ion source of the IRMS. After completion of the EQ peak, the sample tube is processed through bending the cracker, which breaks the scored tube into two pieces releasing the stored gases into the GC carrier. All following steps are identical to the preparation of the EQ peak. Following this alternating EQ-SA scheme, all sample tubes are measured. A final "linearity section" completes the IRMS run to check whether the linearity of the system has changed during the measurement of the samples (not shown in Fig. 5).

## 4 Data processing and correction

### 4.1 Peak integration

To allow for a flexible and transparent peak integration, we use a self developed peak integration routine, similar to the software used by Bock et al. (2010). While the start of the $CO_2$ peak is defined with a slope threshold criterion, the end of the $CO_2$ integral is determined using the first derivative of the *m/z* 44 beam (derivative decreases with the advent of the $N_2O$ peak).

A special feature of our integration procedure is shown in Fig. 6b, which shows the zoomed background region of the $CO_2$ peak. About 90 s before the $CO_2$ peak starts, the background drops by ca. 3 mV in case of *m/z* 44 beam. This step is due to the immersion of the cryofocus in LN2, which collects not only the current $CO_2$/$N_2O$ from the cracker for 90 s, but also a small fraction from the tail of the previous peak. To account for this collected background, we calculate the "background area" for each beam and subtract this area from the proper peak area. Although this "background area" is small (∼0.3 Vs compared to a *m/z* 44 area 120 Vs for a typical sample peak) and almost constant, correcting for it generally reduces the amount dependency of the $\delta^{13}C$ values, as this constant background area would otherwise add to a variable peak area. Note that it is advantageous that the $CO_2$ of the $CO_2$-$N_2O$ mixture has a similar $\delta^{13}C$ value to the $\delta^{13}C$ of ice core samples, in our case −4.48 ‰ compared to the sample range of typically −6 ‰ to −7 ‰, thus, minimizing the influence of a peak-to-peak contamination.

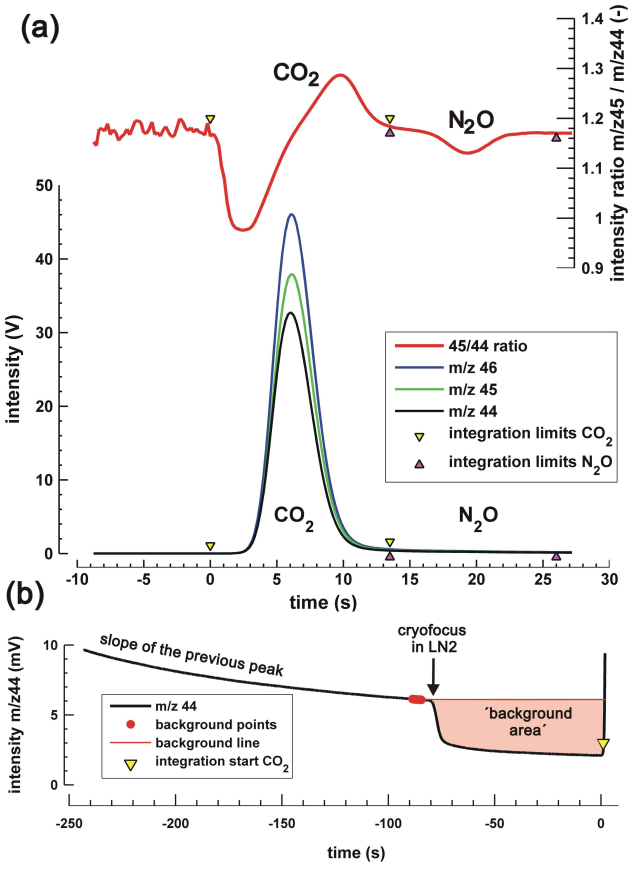


**Fig. 6.** **(a)** Sample chromatogram showing the separation of $CO_2$ from $N_2O$ for an ice core sample. The $N_2O$ peak is clearly visible in the measured *m/z* 45/44 beam ratio as a negative bump since the average molecular mass of $N_2O$ is lower than that of $CO_2$. However, as the typical atmospheric abundance of $N_2O$ is only 1/1000 of $CO_2$, the $N_2O$ peak is not visible in the intensity plot below. **(b)** Zoom into the region prior to the $CO_2$ peak start to illustrate the background in front of the peak. The background is determined around 85 s before the peak start.

To calculate the peak area for $N_2O$, only the beam *m/z* 44 is used, since we do not calculate isotope ratios. As the $N_2O$ peak sits on the shoulder of the ca. 1000 fold larger $CO_2$ peak, the background correction is a critical step in determining the $N_2O$ peak area. From the start of the $N_2O$ peak backwards we take 10 s from the $CO_2$ tail and 5 s after the end of the $N_2O$ peak. An exponential fit is calculated covering those background points before and after the $N_2O$ peak. Using this fit, the $N_2O$ peak is separated from the $CO_2$ peak and its area is integrated.

### 4.2 Referencing strategies and $\delta^{13}C$ corrections

Motivated by the identical treatment principle, we apply the following hierarchic referencing and correction strategy analogue to Behrens et al. (2008) to account for drift and fractionation processes throughout the entire system.

1. $CO_2$ pulses of our monitoring gas are introduced by the reference port of the GP box at the beginning and at the end of a GC-IRMS measurement run (Fig. 5). These on/off pulses are used to monitor a drift in the isotope ratios or the beam intensity of the IRMS during the measurement run. These pulses cannot be used for any drift correction as they are admitted only at the start and end of the measurement, but they are helpful for troubleshooting and excluding errors in the IRMS source.

2. $CO_2/N_2O$ mixtures injected to the cracker system are used twofold. First, to correct for the temporal $\delta^{13}C$ drift caused by instability of the mass spectrometer itself, changing water levels, but also due to equilibration/saturation processes of the GC column occurring during the measurement time of $>15$ h ("drift correction"). Secondly, to provide the empirical relationship of the $m/z\,44$ peak area to the $\delta^{13}C$ value ("linearity correction"), with which the amount dependency of the $\delta^{13}C$ values is corrected for.

3. Air reference samples processed with the sublimation system are the final reference basis for $\delta^{13}C$ and the mixing ratios of $CO_2$ and $N_2O$. Currently, we apply a "1-point calibration" using the results from the Boulder 2 cylinder, which is isotopically sufficiently close to our ice core samples. Within each GC-IRMS measurement run consisting of approximately 30 ice core samples, four to five of these air samples are randomly measured.

Therefore, the following data processing and correction scheme is applied on the raw $\delta^{13}C$ results of the peak integration routine. In a first step, the mean of the air reference samples is set to the assigned values of the cylinder. The next step is to correct for a $\delta^{13}C$ drift during the measurement run. Using all EQ peaks during the whole run, a cubic spline interpolation is performed and applied to all measured peaks types (EQ, L1-L3, and SA). Typically, the drift is on the order of 0.04 ‰ $h^{-1}$. After this trend correction, the area-$\delta^{13}C$ relationship from three different peak sizes (L1, L2, L3) is calculated and all measured peaks are corrected for "linearity" effects (Hall et al., 1999; Schmitt et al., 2003). The typical slope of the area-$\delta^{13}C$ function is 0.002 ‰ $Vs^{-1}$. For ice core samples, ranging between 120 Vs for interglacial $CO_2$ values to 80 Vs for glacial values, this translates to a correction of maximum 0.08 ‰. After these corrections, the mean value of the air reference peaks is adjusted again to the assigned value of the cylinder, thus, referencing all peaks of the measurement run with respect to Boulder 2. The referencing and correction strategy for $\delta^{13}C$ presently relies only on a 1-point calibration. Additionally, the $\delta^{13}C$ values of the reference cylinders are 1–2 ‰ more negative than the typical ice core samples we measure. These two shortcomings onto the measurement accuracy can be improved in the future using two air standards with $\delta^{13}C$ values that bracket the $\delta^{13}C$ values of the ice core samples.

## 5 Procedure verification and comparison

### 5.1 Measurement reproducibility

In the following, we discuss the measurement precision of the system, starting with the $CO_2/N_2O$ pulses admitted to the cracker-GC-IRMS, followed by the air reference samples processed with the sublimation system and finally the ice core samples. The results are summarised in Table 1. As can be seen for the $CO_2/N_2O$ injections, the precision for $\delta^{13}C$ depends on the peak size, with 1 $\sigma$ standard deviation of the small "L1" peaks of 0.05 ‰ compared to 0.03 ‰ for the three times larger "L3" peaks. While for dual-inlet IRMS the measurement precision can be close to the theoretical shot noise limit (Merritt et al., 1995), for continuous flow-IRMS the precision is limited rather by the more complex sample preparation and the GC system. The precision of our air reference gases Boulder 1 and 2 processed with the sublimation system is 0.05 ‰ and 0.04 ‰, thus, comparable to that of the $CO_2/N_2O$ pulses. Therefore, the additional error from the gas processing in the sublimation system is small. During the last two years, several samples from different ice cores at different depth intervals were measured in replicate. These measurement precisions are compared in Table 1 as well. Overall, the precision ranges between 0.04 ‰ and 0.08 ‰, which is slightly lower than the precision for the reference gases. This is not surprising as additional effects can contribute to the variance of ice core samples. Notably chemical reactions of impurities within the ice core sample or during the sublimation, physical fractionation processes during the bubble close-off from the firn air and also processes during the drilling and storage of the ice core can alter the $\delta^{13}C$ composition. It is beyond the scope of this paper to discuss all these effects, nor does the current data basis yet allow firm conclusions, but there is indication that ice from the Talos Dome ice core is more reliable than from other cores. One hint for its "good ice quality" might be that its inorganic impurity content during the glacial is much lower compared to the other Antarctic ice cores (Delmonte et al., 2010), reducing the likelihood for chemical reactions and in-situ production of minute amounts of $CO_2$. This feature of the coastal Talos Dome ice core can be observed as well for new $N_2O$ mixing ratio measurements recently obtained (Schilt et al., 2010), which showed no clear signs of in situ $N_2O$ production in contrast to other ice cores, like the inland cores EDML or EDC. However, besides these observations, there is no proven causal link between Talos Dome's low impurity concentration, missing $N_2O$ insitu production and its slightly better reproducibility of $CO_2$ and $\delta^{13}C$ measurements. More work is necessary and underway on these issues. As expected

**Table 1.** The table shows the average reproducibility (1-$\sigma$ standard deviation) for measurements of calibrated air samples (Boulder 1 and 2 cylinders) and ice core samples for the parameters $\delta^{13}C$, and the mixing ratios of $CO_2$ and $N_2O$. Ice measurements were done on three different Antarctic ice cores, two EPICA drill sites (European Project for Ice Coring in Antarctica), EPICA-Dome C, or EDC, (at the Dome C drill site) and EPICA-DML (drill site at Dronning Maud Land), or EDML and the Talos Dome ice core, TALDICE. From these different cores, different depth ranges were analysed providing a range of physical and chemical ice properties. The column "*n*" denotes the number of replicates per sample. Column "*m*" denotes the total number of samples, where replicates have been measured. Note that for $CO_2$/$N_2O$ pulses no $CO_2$ and $N_2O$ mixing ratios can be derived using our volumetric method.

| Type of measurement | $CO_2$ peak size (nmol) | *n* | *m* | $\delta^{13}C$ 1 $\sigma$ (‰) | $CO_2$ 1 $\sigma$ (ppmv) | $N_2O$ 1 $\sigma$ (ppmv) |
|---|---|---|---|---|---|---|
| $CO_2$/$N_2O$ pulses (L1) | 8 | | 50 | 0.05 | – | – |
| $CO_2$/$N_2O$ pulses (L2) | 16 | | 50 | 0.04 | – | – |
| $CO_2$/$N_2O$ pulses (L3) | 24 | | 50 | 0.03 | – | – |
| "Boulder 1" CA06195 | 16 | 4 | 3 | 0.050 | 0.9 | 1.6 |
| "Boulder 2" CA06818 | 26 | 4 | 12 | 0.037 | 1.3 | 6.9 |
| bubble ice EDC (100 m–600 m) | 16–24 | 3 | 28 | 0.061 | 1.9 | 8.6 |
| clathrate ice EDC (>1200 m) | 16–24 | 3 | 27 | 0.082 | 2.6 | 9.9 |
| mixing zone Talos (600 m–1200 m) | 16–20 | 3 | 4 | 0.036 | 1.5 | 8.9 |
| clathrate ice Talos (>1200 m) | 18–24 | 3 | 15 | 0.048 | 2.6 | 8.2 |
| clathrate ice EDML (>1200 m) | 18–24 | 3 | 8 | 0.053 | 1.8 | 18.1 |

when using a quantitative extraction technique, ice samples from the difficult bubble-clathrate mixing zone can be measured for $\delta^{13}C$ and the $CO_2$ mixing ratio as reproducible as samples from the bubble ice zone or fully clathrated samples (Fig. 1).

The precision for the mixing ratios for the air references and the ice cores are shown in Table 1. For $CO_2$ we obtain an average 1 $\sigma$ precision of ca. 1 ppmv for the air references and 2–3 ppmv for the different ice cores. This precision is comparable to the precision of mechanical extraction techniques and other studies using sublimation (Etheridge et al., 1996; Güllük et al., 1998; Siegenthaler et al., 2005b; Ahn et al., 2009; Lourantou et al., 2010a; Lüthi et al., 2010). For $N_2O$ we obtain a precision for reference air sample between 1.6 ppbv and 6.9 ppbv, and between 8.2 ppbv and 18.1 ppbv for the different ice cores. As pointed out above, most glacial sections of Antarctic and Greenland ice cores show problems with in situ $N_2O$ production at certain age intervals. Therefore, the high scatter observed for EDML is at least in part due to the internal variability of the ice rather than an analytic problem. For the Talos Dome ice core we obtain a precision of 8–9 ppbv, which is a little less precise compared to the range of 5–6 ppbv obtained by others (Sowers et al., 2003; MacFarling Meure et al., 2006; Schilt et al., 2010).

If required, the precision for the mixing ratios can be improved further. As the primary focus of this new technique lies in high-precision $\delta^{13}C$ measurements, the devices and measurement procedure was optimised for $\delta^{13}C$, with the mixing ratios being 2nd priority. The main source of uncertainty in the mixing ratio results from flow changes in the cracker-GC-IRMS system, which translates into changes in peak size. This behaviour is visible in Fig. 5, where the amplitude of the "EQ" and "L3" peaks slightly increases between 200 min and 300 min. Although this does not affect the $\delta^{13}C$ values, it directly translates into the precision of the mixing ratios.

### 5.2 Comparison with previous ice core results

While determining the precision of a new method is relatively easy, it is more troublesome to quantify the accuracy. This is especially true for ice core analytics since properties like extraction behaviour of the ice sample can substantially differ from the reference material, typically a cylinder with pressurised air. The general practise for well mixed atmospheric gases is to compare results obtained with different methods from different ice cores. If the results agree within their errors there is confidence that the results represent the correct past atmospheric composition. Figure 7 provides a comparison of our results with measurements of previous studies using different extraction principles and measurement techniques. For $\delta^{13}C$ we compare our sublimation data with results using a dry extraction (Elsig et al., 2009). The mean of all 65 differences is 0.014 ‰ with a 1 $\sigma$ standard deviation of 0.095 ‰, thus, no significant differences between the two methods for bubble ice within their error limits exist (Fig. 7a). For the $CO_2$ mixing ratio, a depth interval of the EDC core with bubble ice was selected for this comparison as only here the efficiency of the mechanical extraction is sufficiently high (typically around 80 %). Additionally, this interval covers a wide range of $CO_2$ concentrations between 185 ppmv and 265 ppmv (2001). Here, the mean difference

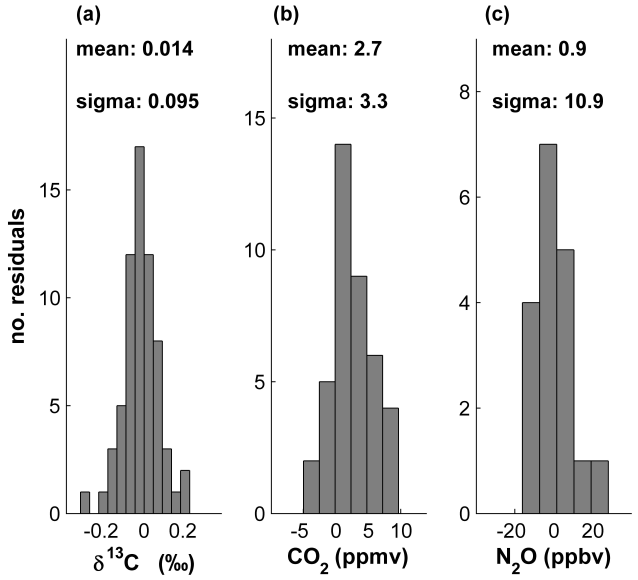


**Fig. 7. (a)** Comparison of $\delta^{13}C$ results obtained with the sublimation technique with results using a mechanical extraction device on the same ice core (Elsig et al., 2009). Shown are the differences between the sublimation and the results of the mechanical extraction device measured on the EDC ice core over the depth interval from 110 m to 580 m (bubble ice). Differences were calculated where both methods measured neighbouring ice samples, which have air occluded which can be regarded identical for this purpose (mean age differences < 25 years), when taking the averaging effect of the bubble enclosure process into account. **(b)** Comparison of $CO_2$ concentration measurements obtained with our sublimation system with published data from the same ice core using a mechanical extraction device (Monnin et al., 2001). Within the covered depth range the air is exclusively trapped in bubbles ("bubble ice"). The measured depth interval covers the time interval of the last deglaciation, thus, covers $CO_2$ concentrations between 185 and 265 ppmv, i.e. almost the full range of the glacial/interglacial $CO_2$ variability. **(c)** Comparison of $N_2O$ concentration measurements obtained with our sublimation system with published data from the same ice core using a melt extraction device (Schilt et al., 2010). At this depth range, the bubbles have transformed into clathrate hydrates ("clathrate ice"). The selected time interval (65–90 ka) includes rapid $N_2O$ variations between 210 and 265 ppmv, thus, covers almost the full natural variability during the last 800 ka.

between the methods is 2.7 ppmv with a $1\,\sigma$ of 3.3 ppmv. The same holds for $N_2O$, where we compared our data with recent measurements on Talos Dome ice. Here, the mean difference is only 0.9 ppbv, with a $1\,\sigma$ of 10.9 ppbv.

A second approach to assess the accuracy of gas reconstructions from ice cores is to provide a temporal overlap between atmospheric measurements, firn air measurements and air trapped in ice. This approach requires a special setting, like an ice core drill site with a very high accumulation rate where air from recent decades is enclosed. These conditions were fulfilled in studies by Etheridge et al. (1996), Francey et al. (1999), and MacFarling Meure (2006), using ice from the Law Dome ice cores, which overlap with firn air measurements and direct atmospheric samples from the Cape Grim Air Archive. A temporal overlap between archived air, firn air and air extracted from ice was accomplished for the year 1978, where all three archives provided data. However, due to age spread within the firn column of about 12.5 years (Francey et al., 1999), the ultimate precision of the temporal match is set by the age spread of the firn air. These studies convincingly showed that their $CO_2$ and $\delta^{13}C$ measurements on these ice cores match their firn air measurements, and the archived air samples within the combined measurement uncertainty. In a recent publication (Elsig et al., 2009) we could demonstrate that our data is in agreement with the ice core results by Francey et al. (1999), which verifies our results in terms of accuracy. We acknowledge, that due to the large age spread of the EDC core (about 170 years for Holocene conditions; Spahni et al., 2003) the comparison with the decadally resolved Law Dome record cores is challenging given the observed $\delta^{13}C$ trend during this interval in the Law Dome record. A tighter connection of our $\delta^{13}C$ ice core measurement with the Law Dome-air archive link could be established by remeasuring Law Dome ice with our system.

## 6 Conclusions

We have presented an analysis system capable of high precision measurements of $\delta^{13}C$ on $CO_2$ on ice core samples. When both the ice quality, such as samples from Talos Dome, and the measurement conditions are optimal then we obtain for $\delta^{13}C$ measurements a $1\,\sigma$ precision for neighbouring samples of usually 0.05 ‰. Given the typical long term variations of atmospheric $\delta^{13}C$ during the late Pleistocene of 0.5 ‰, this precision allows for analyses with a signal to noise ratio of 10, thus, sufficient to provide key constraints for biogeochemical models. Our system uses for the first time a sublimation technique, allowing a quantitative extraction for gases trapped in ice core samples. Additionally, the mixing ratios of $CO_2$ and $N_2O$ can be derived with a precision of 2 ppmv and 8 ppbv, respectively, similar to conventional extraction systems. The various cold traps of the analysis system are equipped with cooling systems using liquid nitrogen regulated by controllers, allowing a highly automated system free of organic solvents.

The performance of the system was tested on a variety of Antarctic ice cores and different ice properties ranging from bubble ice, ice from the bubble/clathrate transition zone and fully clathrated ice proving the reliability and very high precision of our new method. With the 100 % extraction efficiency of our sublimation method we have now for the first time an extraction at hand that ensures unfractionated, high-precision $\delta^{13}CO_2$ analyses also in partially or fully clathrated ice. This opens the window to the $\delta^{13}CO_2$ archive in central Antarctic ice from depths greater than about 700 m, where clathrate formation begins. For instance in the EPICA

Dome C ice core these depths correspond to the time interval from 25 000 to 800 000 yr BP, i.e. the major part of the entire ice core record. The same applies for $CO_2$ concentration measurements on clathrated ice, where our new sublimation technique can act as a reference method for the mechanical extraction techniques.

*Acknowledgements.* We thank Hinrich Schäfer and the second anonymous reviewer for their very constructive and detailed comments which helped to improve the paper. This work is a contribution to the "European Project for Ice Coring in Antarctica" (EPICA), a joint European Science Foundation/European Commission (EC) scientific program, funded by the EC under the Environment and Climate Program and by national contributions from Belgium, Denmark, France, Germany, Italy, The Netherlands, Norway, Sweden, Switzerland, and UK. This is an EPICA publication. Funding by the German Ministry of Education and Research (BMBF) through the German climate research program DEKLIM (project RESPIC) is acknowledged. The assistance of Melanie Behrens is gratefully acknowledged for running the MS and the organization of the lab at the Alfred Wegener Institute for Polar and Marine Research, Bremerhaven, Germany. We also thank for the technical advice from Klaus-Uwe Richter.

Edited by: A. Hofzumahaus

## References

Ahn, J. and Brook, E. J.: Atmospheric $CO_2$ and climate on millennial time scales during the last glacial period, Science, 322, 83–85, doi:10.1126/science.1160832, 2008.

Ahn, J. H., Brook, E. J., and Howell, K.: A high-precision method for measurement of paleoatmospheric $CO_2$ in small polar ice samples, J. Glaciol., 55, 499–506, 2009.

Anklin, M., Barnola, J.-M., Schwander, J., Stauffer, B., and Raynaud, D.: Processes affecting the $CO_2$ concentrations measured in Greenland ice, Tellus, 47, 461–470, 1995.

Augustin, L., Panichi, S., and Frascati, F.: EPICA Dome C 2 drilling operations: performances, difficulties, results, Ann. Glaciol., 47, 68–72, 2007.

Barnes, P. R. F., Wolff, E. W., Mallard, D. C., and Mader, H. M.: SEM Studies of the Morphology and Chemistry of Polar Ice, Microsc. Res. Tech., 62, 62–69, 2003.

Behrens, M., Schmitt, J., Richter, K.-U., Bock, M., Richter, U., Levin, I., and Fischer, H.: A gas chromatography/combustion/isotope ratio mass spectrometry system for high-precision $\delta^{13}C$ measurements of atmospheric methane extracted from ice core samples, Rapid. Commun. Mass Spectrom., 22, 3261–3269, doi:10.1002/rcm.3720, 2008.

Bock, M., Schmitt, J., Behrens, M., Möller, L., Schneider, R., Sapart, C., and Fischer, H.: A gas chromatography/pyrolysis/isotope ratio mass spectrometry system for high-precision $\delta$D measurements of atmospheric methane extracted from ice cores, Rapid. Commun. Mass Spectrom., 24, 621–633, doi:10.1002/rcm.4429, 2010.

Broecker, W. S. and Clark, E.: Holocene atmospheric $CO_2$ increase as viewed from the seafloor, Global Biogeochem. Cy., 17, 1052, doi:10.1029/2002GB001985, 2003.

Brovkin, V., Hofmann, M., Bendtsen, J., and Ganopolski, A.: Ocean biology could control atmospheric $\delta^{13}C$ during glacial-interglacial cycle, Geochem. Geophy. Geosy., 3, 1–15, doi:10.1029/2001GC000270, 2002.

Caldwell, W. E., Odom, J. D., and Williams, D. F.: Glass-Sample Tube Breaker, Anal. Chem., 55, 1175–1176, 1983.

Delmonte, B., Baroni, C., Andersson, P. S., Schoberg, H., Hansson, M., Aciego, S., Petit, J. R., Albani, S., Mazzola, C., Maggi, V., and Frezzotti, M.: Aeolian dust in the Talos Dome ice core (East Antarctica, Pacific/Ross Sea sector): Victoria Land versus remote sources over the last two climate cycles, J. Quaternary Sci., 25, 1327–1337, doi:10.1002/jqs.1418, 2010.

Des Marais, D. J. and Hayes, J. M.: Tube Cracker for Opening Glass-Sealed Ampoules under Vacuum, Anal. Chem., 48, 1651–1652, 1976.

Elsig, J.: New insights into the global carbon cycle from measurements of $CO_2$ stable isotopes: methodological improvements and interpretation of a new EPICA Dome C ice core $\delta^{13}C$ record, Dissertation, University of Bern, Bern, 2009.

Elsig, J. and Leuenberger, M. C.: C-13 and O-18 fractionation effects on open splits and on the ion source in continuous flow isotope ratio mass spectrometry, Rapid. Commun. Mass Spectrom., 24, 1419–1430, doi:10.1002/rcm.4531, 2010.

Elsig, J., Schmitt, J., Leuenberger, D., Schneider, R., Eyer, M., Leuenberger, M., Joos, F., Fischer, H., and Stocker, T. F.: Stable isotope constraints on Holocene carbon cycle changes from an Antarctic ice core, Nature, 461, 507–510, doi:10.1038/nature08393, 2009.

Etheridge, D. M., Pearman, G. I., and de Silva, F.: Atmospheric trace-gas variations as revealed by air trapped in an ice core from Law Dome, Antarctica, Ann. Glaciol., 10, 28–33, 1988.

Etheridge, D. M., Steele, L. P., Langenfelds, R. L., Francey, R. J., Barnola, J.-M., and Morgan, V. I.: Natural and anthropogenic changes in atmospheric $CO_2$ over the last 1000 years from air in Antarctic ice and firn, J. Geophys. Res., 101, 4115–4128, 1996.

Eyer, M.: Highly resolved $\delta^{13}C$ measurements on $CO_2$ in air from Antarctic ice cores, Dissertation, University of Bern, Bern, 2004.

Ferretti, D. F., Lowe, D. C., Martin, R. J., and Brailsford, G. W.: A new gas chromatograph-isotope ratio mass spectrometry technique for high-precision, $N_2O$-free analysis of $\delta^{13}C$ and $\delta^{18}O$ in atmospheric $CO_2$ from small air samples, J. Geophys. Res., 105, 6709–6718, 2000.

Fischer, H., Wahlen, M., Smith, J., Mastroianni, D., and Deck, B.: Ice core records of atmospheric $CO_2$ around the last three glacial terminations, Science, 283, 1712–1714, 1999.

Francey, R. J., Allison, C. E., Etheridge, D. M., Trudinger, C. M., Enting, I. G., Leuenberger, M., Langenfelds, R. L., Michel, E., and Steele, L. P.: A 1000-year high precision record of $\delta^{13}C$ in atmospheric $CO_2$, Tellus B, 51, 170–193, 1999.

Güllük, T., Slemr, F., and Stauffer, B.: Simultaneous measurement of $CO_2$, $CH_4$, and $N_2O$ in air extracted by sublimation from Antarctica ice cores: Confirmation of the data obtained using other extraction techniques, J. Geophys. Res., 103, 15971–15978, 1998.

Hall, J. A., Barth, J. A. C., and Kalin, R. M.: Routine Analysis by High Precision Gas Chromatography/Mass Selective Detector/Isotope Ratio Mass Spectrometry to 0.1 Parts Per Mil, Rapid. Commun. Mass Spectrom., 13, 1231–1236, 1999.

Ikeda, T., Fukazawa, H., Mae, S., Pepin, L., Duval, P., Champagnon, B., Lipenkov, V. Y., and Hondoh, T.: Extreme fractionation of gases caused by formation of clathrate hydrates in Vostok Antarctic ice, Geophys. Res. Lett., 26, 91–94, 1999.

Indermühle, A., Stocker, T. F., Joos, F., Fischer, H., Smith, H. J., Wahlen, M., Deck, B., Mastroianni, D., Tschumi, J., Blunier, T., Meyer, R., and Stauffer, B.: Holocene carbon-cycle dynamics based on $CO_2$ trapped in ice at Taylor Dome, Antarctica, Nature, 398, 121–126, 1999.

Kawamura, K., Nakazawa, T., Aoki, S., Sugawara, S., Fujii, Y., and Watanabe, O.: Atmospheric $CO_2$ variations over the last three glacial-interglacial climatic cycles deduced from the Dome Fuji deep ice core, Antarctica using a wet extraction technique, Tellus B, 55, 126–137, 2003.

Köhler, P. and Fischer, H.: Simulating changes in the terrestrial biosphere during the last glacial/interglacial transition, Global Planet. Change, 43, 33–55, 2004.

Leckrone, K. J. and Hayes, J. M.: Efficiency and Temperature Dependence of Water Removal by Membrane Dryers, Anal. Chem., 69, 911–918, 1997.

Leckrone, K. J. and Hayes, J. M.: Water-Induced Errors in Continuous-Flow Carbon Isotope Ratio Mass Spectrometry, Anal. Chem., 70, 2737–2744, 1998.

Leuenberger, M., Siegenthaler, U., and Langway, C. C.: Carbon isotope composition of atmospheric $CO_2$ during the last ice age from an Antarctic ice core, Nature, 357, 488–490, 1992.

Leuenberger, M. C., Eyer, M., Nyfeler, P., Stauffer, B., and Stocker, T. F.: High-resolution $\delta^{13}C$ measurement on ancient air extracted from less than 10 $cm^3$ of ice, Tellus B, 55, 138–144, 2003.

Lourantou, A., Chappellaz, J., Barnola, J. M., Masson-Delmotte, V., and Raynaud, D.: Changes in atmospheric $CO_2$ and its carbon isotopic ratio during the penultimate deglaciation, Quaternary Sci. Rev., 29, 1983–1992, doi:10.1016/j.quascirev.2010.05.002, 2010a.

Lourantou, A., Lavric, J. V., Köhler, P., Barnola, J. M., Paillard, D., Michel, E., Raynaud, D., and Chappellaz, J.: Constraint of the $CO_2$ rise by new atmospheric carbon isotopic measurements during the last deglaciation, Global Biogeochem. Cy., 24, 1–15, doi:10.1029/2009GB003545, 2010b.

Lüthi, D., Le Floch, M., Bereiter, B., Blunier, T., Barnola, J. M., Siegenthaler, U., Raynaud, D., Jouzel, J., Fischer, H., Kawamura, K., and Stocker, T. F.: High-resolution carbon dioxide concentration record 650,000–800,000 years before present, Nature, 453, 379-382, doi:10.1038/nature06949, 2008.

Lüthi, D., Bereiter, B., Stauffer, B., Winkler, R., Schwander, J., Kindler, P., Leuenberger, M., Kipfstuhl, S., Capron, E., Landais, A., Fischer, H., and Stocker, T. F.: $CO_2$ and $O_2/N_2$ variations in and just below the bubble-clathrate transformation zone of Antarctic ice cores, Earth Planet. Sc. Lett., 297, 226–233, doi:10.1016/j.epsl.2010.06.023, 2010.

MacFarling Meure, C., Etheridge, D., Trudinger, C., Steele, P., Langenfelds, R., van Ommen, T., Smith, A., and Elkins, J.: Law Dome $CO_2$, $CH_4$ and $N_2O$ ice core records extended to 2000 years BP, Geophys. Res. Lett., 33, L14810, doi:10.1029/2006GL026152, 2006.

Meier-Augenstein, W.: A Reference Gas Inlet Module for Internal Isotopic Calibration in High Precision Gas-Chromatography, Rapid. Commun. Mass Spectrom., 11, 1775–1780, 1997.

Meier-Augenstein, W.: Review: Applied gas chromatography coupled to isotope ratio mass spectrometry, J. Chromat. A, 842, 351–371, 1999.

Meier-Augenstein, W., Watt, P., and Langhans, C.: Influence of Gas Chromatographic Parameters on Measurement of $^{13}C/^{12}C$ Isotope Ratios by Gas-Liquid Chromatography-Combustion Isotope Ratio Mass spectrometry, J. Chromat. A, 752, 233–241, 1996.

Merritt, D. A., Freeman, K. H., Ricci, M. P., Studley, S. A., and Hayes, J. M.: Performance and Optimization of a Combustion Interface for Isotope Ratio Monitoring Gas Chromatography/Mass Spectrometry, Anal. Chem., 67, 2461–2473, 1995.

Monnin, E., Indermühle, A., Dällenbach, A., Flückiger, J., Stauffer, B., Stocker, T. F., Raynaud, D., and Barnola, J.-M.: Atmospheric $CO_2$ concentration over the last termination, Science, 291, 112–114, 2001.

Petit, J. R., Jouzel, J., Raynaud, D., Barkov, N. I., Barnola, J.-M., Basile, I., Bender, M., Chappellaz, J., Davis, M., Delaygue, G., Delmotte, M., Kotlyakov, V. M., Legrand, M., Lipenkov, V. Y., Lorius, C., Pepin, L., Ritz, C., Saltzman, E., and Stievenard, M.: Climate and atmospheric history of the past 420,000 years from the Vostok ice core, Antarctica, Nature, 399, 429–436, 1999.

Ribas-Carbo, M., Still, C., and Berry, J.: Automated system for simultaneous analysis of $^{13}C$, $^{18}O$ and $CO_2$ concentrations in small air samples, Rapid. Commun. Mass Spectrom., 16, 339–345, doi:10.1002/rcm.582, 2002.

Rice, A. L., Gotoh, A. A., Ajie, H. O., and Tyler, S. C.: High-precision continuous-flow measurement of $\delta^{13}C$ and $\delta D$ of atmospheric $CH_4$, Anal. Chem., 73, 4104–4110, 2001.

Schaefer, H., Lourantou, A., Chappellaz, J., Lüthi, D., Bereiter, B., and Barnola, J.-M.: On the suitability of partially clathrated ice for analysis of concentration and $\delta^{13}C$ of palaeoatmospheric $CO_2$, Earth Planet. Sc. Lett., 307, 334–340, doi:10.1016/j.epsl.2011.05.007, 2011.

Schilt, A., Baumgartner, M., Schwander, J., Buiron, D., Capron, E., Chappellaz, J., Loulergue, L., Schüpbach, S., Spahni, R., Fischer, H., and Stocker, T. F.: Atmospheric nitrous oxide during the last 140,000 years, Earth Planet. Sc. Lett., 300, 33–43, doi:10.1016/j.epsl.2010.09.027, 2010.

Schmitt, J., Glaser, B., and Zech, W.: Amount-dependent isotopic fractionation during compound-specific isotope analysis, Rapid. Commun. Mass Spectrom., 17, 970–977, doi:10.1002/rcm.1009, 2003.

Schmitt, J.: A sublimation technique for high-precision $\delta^{13}C$ on $CO_2$ and $CO_2$ mixing ratio from air trapped in deep ice cores, Dissertation, University of Bremen, available at: http://elib.suub.uni-bremen.de/diss/docs/00010568.pdf (last access: July 2011), 2006.

Siegenthaler, U.: $CO_2$-Konzentrationsmessungen an polaren Eisbohrkernen und Tests mit einer neuen Extraktionsmethode, Diplomarbeit, Bern, unpublished, 2002.

Siegenthaler, U., Monnin, E., Kawamura, K., Spahni, R., Schwander, J., Stauffer, B., Stocker, T. F., Barnola, J.-M., and Fischer, H.: Supporting evidence from the EPICA Dronning Maud Land ice core for atmospheric $CO_2$ changes during the past millennium, Tellus, 57, 51–57, 2005a.

Siegenthaler, U., Stocker, T. F., Monnin, E., Lüthi, D., Schwander, J., Stauffer, B., Raynaud, D., Barnola, J. M., Fischer, H., Masson-Delmotte, V., and Jouzel, J.: Stable carbon cycle-climate relationship during the late Pleistocene, Science, 310, 1313,

doi:10.1126/science.1120130, 2005b.

Smith, H. J., Fischer, H., Wahlen, M., Mastroianni, D., and Deck, B.: Dual modes of the carbon cycle since the Last Glacial Maximum, Nature, 400, 248–250, 1999.

Sowers, T., Alley, R. B., and Jubenville, J.: Ice core records of atmospheric $N_2O$ covering the last 106,000 years, Science, 301, 945–948, 2003.

Spahni, R., Schwander, J., Fluckiger, J., Stauffer, B., Chappellaz, J., and Raynaud, D.: The attenuation of fast atmospheric $CH_4$ variations recorded in polar ice cores, Geophys. Res. Lett., 30, 11, doi:10.1029/2003GL017093, 2003.

Trudinger, C. M., Enting, I. G., Francey, R. J., Etheridge, D. M., and Rayner, P. J.: Long-term variability in the global carbon cycle inferred from a high precision $CO_2$ and $\delta^{13}$C-ice-core record, Tellus, 51, 233–248, 1999.

Werner, R. A. and Brand, W. A.: Referencing strategies and techniques in stable isotope ratio analysis, Rapid. Commun. Mass Spectrom., 15, 501–519, 2001.

Wilson, A. T. and Long, A.: New approaches to $CO_2$ analysis in polar ice cores, J. Geophys. Res., 102, 26601–26606, 1997.

Zhang, J., Quay, P. D., and Wilbur, D. O.: Carbon isotope fractionation during gas-water exchange and dissolution of $CO_2$, Geochim. Cosmochim. Acta, 59, 107–114, 1995.

Zumbrunn, R., Neftel, A., and Oeschger, H.: $CO_2$ measurements on 1-$cm^3$ ice samples with IR laserspectrometer (IRLS) combined with a new dry extraction device, Earth Planet. Sc. Lett., 60, 318–324, 1982.